A Novel Automated Planning Approach for Multi-Anatomical Sites Cancer in Raystation Treatment Planning System

ZhaoYang Lou
Affiliated Cancer Hospital of Zhengzhou University, Henan Cancer Hospital
RongHu Mao
Affiliated Cancer Hospital of Zhengzhou University, Henan Cancer Hospital
DingJie Li
Affiliated Cancer Hospital of Zhengzhou University, Henan Cancer Hospital
LingLing Tian
Affiliated Cancer Hospital of Zhengzhou University, Henan Cancer Hospital
Bing Li
Affiliated Cancer Hospital of Zhengzhou University, Henan Cancer Hospital
HongChang Lei
Affiliated Cancer Hospital of Zhengzhou University, Henan Cancer Hospital
Hong Ge (gehong616@126.com)
Affiliated Cancer Hospital of Zhengzhou University, Henan Cancer Hospital

Research Article

Keywords: automated planning, Raystation, multi-anatomical sites cancer, dose prediction,beam angle optimization, scripting

Posted Date: March 10th, 2022

DOI: https://doi.org/10.21203/rs.3.rs-1427022/v1

Abstract

Background

Previous automated planning approach studies for Raystation were limited to a specific anatomical site cancer or a single treatment technique. The purpose of this study is to develop an automated planning approach in Raystation and evaluate its feasibility and performance in multiple clinical application scenarios.

Methods

Sixty patients, including 20 nasopharyngeal carcinoma (NPC), 20 esophageal carcinoma (ESCA) and 20 rectal cancer (RECA), who were treated with volumetric-modulated arc therapy for NPC and RECA and intensity-modulated radiotherapy for ESCA, were retrospectively enrolled in this study. An automated planning approach (Ruiplan), consisting of five key modules: prescription and OAR identification module, auxiliary structure generation module, dose prediction and objectives setting module, beam configuration module, plan fine-turning module, was developed by using the scripting platform of Raystation. Radiotherapy plans were re-generated both automatically by using Ruiplan and manually by experienced physicists. Target coverage, organs at risk (OARs) sparing, and planning efficiency of the automated plans (APs) and manual plans (MPs) were statistically compared using paired student *t*-test.

Results

For target coverage, APs yielded superior dose homogeneity in NPC and RECA, compared to MPs, while maintaining similar dose conformity for all studied anatomical sites. For OARs sparing, APs led to significant improvement in most OARs sparing, compared to MPs. The max dose of the lens, eyes and optic nerves in NPC, the V20 and mean dose of lungs, the V30, V40 and mean dose of heart in ESCA, the V30, V50 of bowel and V30 of femoral heads in CRCA were significantly decreased on average in APs compared to MPs ($P < 0.05$). The average planning time required for APs was reduced by more than 43% compared with MPs. Despite the increased monitor units (MUs) for NPC and RECA in APs, the beam-on time of APs and MPs had no statistical difference. Both the MUs and beam-on time of APs were significantly lower than that of MPs in ESCA ($P < 0.05$).

Conclusions

The developed Ruiplan was capable of generating high-quality treatment plans that were comparable to the MPs created by experienced physicists, in a variety of treatment techniques and cancer sites studied.

Brackground

Over the past two decades, significant advances in planning and delivery of radiotherapy have been accomplished, the sophisticated intensity-modulated radiation therapy (IMRT) and the volumetric-modulated arc therapy (VMAT) treatment techniques are widely used in the field of radiotherapy. Owing to the superior dose modulation capability, these techniques are able to improve dose distribution and conformity, reduce irradiation to normal tissues and thereby minimize the risk of toxicity. However, the treatment planning process is time-consuming, a successful inverse planning of radiotherapy treatment relies on tweaking of a number of parameters, complex treatment planning with IMRT or VMAT remains challenging in order to achieve clinically acceptable plans [1].

In order to improve the quality and consistency of treatment plans, there is a growing body of literature investigating capability of automated planning algorithm, which can be generally divided into two approaches, based on the planning optimization strategy: Atlas-based, Template-based. For the atlas-based planning optimization strategy, it relies on a predictive model built on statistical analysis of a group of previous plans [2–5]. A new treatment plan is then created by comparing targets and organs at risk (OARs) anatomy with the model and from there derived the dose volume histogram (DVH) objectives. One example of this is the commercial RapidPlan used in the Eclipse treatment planning system (TPS) (Varian Medical Systems, Palo Alto, USA), and various studies have shown that this approach can improve both planning efficiency and plan quality consistency [6–10]. For the template-based planning optimization strategy, it tries to drive the optimization according to template originated from a protocol, mimics the decision-making process of an experienced planner with a progressive optimization algorithm which continually adjusts planning objectives based on the difference between planning goals and current DVH parameters [11–14]. Typical template-based automated planning approaches are Erasmus-iCycle works with Monaco TPS (Elekta AB, Stockholm, Sweden) [15] and the Autoplanning works with Pinnacle^3 TPS (Philips Medical Systems, Fitchburg, WI, USA) [16].

In addition to the commercial automated planning approaches mentioned above, several studies used the scripting function of TPS or external application interface to customize the automated workflow [17–23], For example, based on the Eclipse scripting application programming interface, Morales et al.[19] developed an automated verification planning approach, Lin et al. [20] reported an automated IMRT planning approach for early-stage breast cancer. Based on the scripting module of Pinnacle^3, Xhaferllari et al. [18] and Zhang et al. [21] presented a multi-anatomical sites automated planning strategy respectively. Although the Monaco TPS has no scripting function yet, Ayala et al.[22] have realized the automated IMRT and VMAT planning in Monaco through an open-source software library. Using the scripting platform of Raystation TPS (Raysearch, Stockholm, Sweden), Yang et al. [23] reported an automated planning approach for nasopharyngeal carcinoma.

Although many studies on automated planning have been reported, such studies based on Raystation are still rare, and the previous automated planning approach studies for Raystation were limited to a specific anatomical site cancer or a single treatment technique, such as IMRT or VMAT [23–25]. An automated planning approach for Raystation feasible for multi-anatomical sites caner and multi-treatment

techniques is still missing, and we argue that a well-designed automated planning algorithm can achieve this goal and together with increase of plan quality and efficiency.

In this study, we developed a fully-automated planning approach in Raystation, referred to as Ruiplan, Ruiplan can be used for multi-anatomical sites treatment planning and support multi-treatment techniques. A cohort of 60 patients with nasopharyngeal carcinoma (NPC), esophageal carcinoma (ESCA) and rectal cancer (RECA) who previously received radiotherapy in Henan Cancer Hospital were randomly selected to investigate the feasibility of the approach. These treatment plans were re-planned automatically and manually by Ruiplan and senior physicist, respectively. The dosimetric quality and work efficiency were compared between the automated plans (APs) and manual plans (MPs).

Methods

Description of Automated Planning Approach

The Raystation has an easy-to-use scripting platform, which involved the implementation of IronPython programming language combined with the Microsoft.Net framework. Based on the scripting platform of Raystation (Version 4.7.5), we developed an automated planning approach which named Ruiplan with the characteristic of feasible for multi-treatment techniques and multi-anatomical cancer radiotherapy. The developed Ruiplan consisted of five independent modules: (1) prescription and OAR identification module, (2) auxiliary structure generation module, (3) Dose prediction and objectives setting module, (4) beam configuration module, (5) plan fine turning module. The detailed description of each module is described in the following sections. The structure and workflow of Ruiplan are illustrated in Fig. 1.

Prescription and OAR Identification Module

The identification of prescription and OAR is realized by analyzing structure names. For the target, the planner needs to rename the target in the format of ‘Target_fraction_dose’ before planning, the module will automatically identify the prescription, for example, ‘PTV_25_4500’ means the target PTV prescription fraction number is 25 and prescription dose is 45.00 Gy. This method still applies the case of multiple prescription. For the identification of OARs, a naming list is designed for each OAR based on the report of the American Association of Physicists in Medicine task group No. 263 [26] and the naming habits of clinicians, the module automatically distinguish each OAR by iterating the naming lists.

Auxiliary Structure Generation Module

Durning the planning process, the auxiliary structure contour module automatically generates two kinds of structures, one is the tuning structures including the rings and shells around the targets to control the dose full-off and ensure a better conformity index (CI) and homogeneity index (HI). The other is the planning organs at risk volume structures to drive the OARs sparing.

Dose Prediction and Objectives Setting Module

The dose prediction algorithm used in this study is proposed by Pang et al. [27]. This method considers the contribution of prescription dose and the location relationship between OARs and targets to the adsorbed dose of OARs, the formula is defined as bellow:

$$Y = C_0 + C_{in} \bullet V_{in} + C_1 \bullet V_1 + C_2 \bullet V_2 + \cdots + C_n \bullet V_n$$

1

in which Y predicts the normalized mean dose and the normalized Dn% (Dn% is defined as the dose received by n% of organ volume) for each OAR. V_{in} is the normalized intersection volume of target and the OAR, V_1, V_2 … V_n represent the normalized intersection volume of different rings away from target volume and OAR, C_0, C_{in}, C_1 … C_n are the fitting coefficients. For each OAR, the predicted Y values were fitted to obtain the predicted DVH curves, then based on the predicted curves, the objectives for dose sparing were set for each OAR.

Beam Configuration Module

Aiming at the problem of beam configuration in planning process, we solve it through a user interface which is shown in Additional file Fig. 1, the planner can select beam configuration and other necessary parameters through the user interface. A variety of beam configuration presets are set for different treatment technique, including IMRT, VMAT, SBRT (stereotactic body radiation therapy) and SRS (stereotactic radiosurgery). Once IMRT is adopted, the beam angle optimization (BAO) function is optional to the planner. The workflow of the BAO process is illustrated in Additional file Fig. 2.

Plan Fine-tuning Module

The plan fine-tuning module mimics the planning process of experienced planner with a progressive way. As is shown in Fig. 1, after each cycle of direct machine parameter optimization (DMPO), the fine-tuning module automatically adjust the objectives and generate new auxiliary structures according to the target coverage and OARs sparing. The fine-tuning process automatically stop until converging or achieving the maximum number of preset optimization loop.

Patient Selection and Treatment Planning

Three anatomical sites cancer and two treatment techniques are presented to demonstrate the potential and challenges of Ruiplan with respect to manual planning. From April 2019 to July 2020, a total of 60 patients who received treatment in Henan Cancer Hospital were randomly selected, 20 patients for each of the following pathologies: NPC, ESCA and RECA. None of the patients received radiotherapy prior to the study enrollment, and all were free of distant metastases or contraindications to radiotherapy. According to the American Joint Committee on Cancer (AJCC), for the NPC case, 5 patients had stage II disease, 13 had stage III and 2 had stage IVa. For the ESCA case, 2 patients had stage I, 6 patients had stage II and 12 had stage III. For the CRCA case,5 patients had stage II disease, 14 had stage III and 1 had stage IV. For all the patients, the APs and MPs were generated using 6 MV X-ray beams with a maximum dose rate of 600 monitor unit (MU)/min from the Varian Truebeam linear accelerator. The treatment

techniques used are VMAT for NPC and RECA, IMRT for ESCA. In the VMAT plans, two coplanar full arcs were used in both APs and MPs. For IMRT plans, 5 beam step-and-shot with nonequal beam angle spacing were used, meanwhile BAO function were selected for the APs.

Dose Prescription and Clinical Objectives

The prescribed doses of the three anatomical cancer radiotherapy were as follows: For the NPC case, 60.20 Gy to the PGTV and PGTVnd, 56.00 Gy to the PTV1, 50.40 Gy to the PTV2, all targets were simultaneously irradiated over 28 daily fractions. For the ESCA and RECA cases, 50.40 Gy to the PTV, in 28 fractions. For the three anatomical sites, the clinical acceptability of targets included 100% of radiation dose to cover 95% of the targets volume, and no patients received larger than 110% of the targets prescribed dose. Regarding the OARs, the dose-volume constraints of our clinical protocols are listed in Table 1.

Table 1
Planning objectives for critical structures.

OARs	Objective type	Dose	Volume
Brian stem	Max dose	54 Gy	
Spinal cord	Max dose	45 Gy	
Lens	Max dose	9 Gy	
Eye	Max Dose	30 Gy	
Optic nerves	Max dose	54 Gy	
Chiasma	Max dose	54 Gy	
Parotids	DVH	30 Gy	50%
Lungs	DVH	5 Gy	65%
	DVH	20 Gy	25%
Heart	DVH	30 Gy	40%
	DVH	40 Gy	25%
	Mean Dose	26 Gy	
Bladder	DVH	50 Gy	50%
Bowel	DVH	30 Gy	50%
Femoral heads	Max dose	50 Gy	
	DVH	30 Gy	50%

Plan Evaluation and Analysis

DVH analysis was used for plan comparison, The target volumes analysis included D2%, D98%, HI and CI, and the OARs dose sparing analysis included the maximum dose, mean dose and Vx (Vx is defined as the relative volume of organ receives x Gy dose). The values of D1% was defined as metrics for maximum doses. For each target volume, HI [28] was defined as:

$$HI = \frac{D2\% - D98\%}{D_p}$$

2

where D_p is the prescription dose, the closer the value of HI is to 0, the better is the dose homogeneity.

The CI [29] was defines as:

$$CI = \frac{V_{t,ref}}{V_{ref}} \bullet \frac{V_{t,ref}}{V_t}$$

3

where $V_{t,ref}$ was the target volume covered by the reference isodose, V_{ref} was the volume of the reference isodose and V_t was volume of target. CI ranges from 0 to 1, the ideal value 1 of CI indicates the perfect conformity that the prescription isodose line completely coincides with the target volume.

For the non-tumor tissues, the integral dose (ID) was calculated as the product between mean dose and non-tumor tissue volume (Gy*cc).

Planning and Treatment Efficiency

The time efficiency of manual and automated planning design and implementation was evaluated. For all the patients, total planning time, beam-on time and the total number of MUs were recorded for both MPs and APs. All optimizaiton processes were performed on a local workstation (Dell Precision 7910 Wrokstation, 6-core 3.40 GHz processor, 32GB Memory, Nvidia Quardro K5000 GPU).

Dosimetric Verification

Dosimetric verification for all MPs and APs was carried out by using the ArcCHECK device [30], the ArcCHECK (Sun Nuclear, Melbourne, FL, USA) is a cylindrical water-equivalent phantom with a 3D array of 1386 diode detectors arranged in a spiral pattern, with 10 mm sensor spacing. The comparison between the measured dose and the TPS calculated dose for all plans was performed using gamma analysis, following the suggestions of the AAPM report No. 218 [31], dosimetric verification was considered optimal if the gamma index criteria exceeded 95% with 3%-2mm criteria for dose and distance-to-agreement.

Statistical Analysis

The difference of dose metrics and work efficiency parameters between two group plans were compared and analyzed using paired student *t*-test. All statistical analysis were conducted with SPSS Statistics 19.0 software (IBM, Chicago, IL, USA). The differences were considered statistically significant when $p < 0.05$.

Results

All the APs and MPs fulfilled the criteria for clinical acceptability in terms of target coverage and OARs sparing.

Target Coverage

Table 2 presents the dose metrics for the targets of three anatomical sites. For NPC case, The D2% received by PGTV, PGTVnd and PTV1, the HI of PGTV and PTV1 in the APs is lower (better) than those in MPs ($P < 0.05$). The D98% received by PTV1 and PTV2 in the APs is higher (better) than those in MPs ($P < 0.05$). No significant differences were found for other parameters of the targets. For ESCA case, the PTV coverage for APs and MPs is approximately equal for all parameters with no significant statistical differences. For RECA case, The HI showed statistically significant differences ($p < 0.05$) between the AP and MP group, however only a difference of 0.007 in absolute value, no significant differences were found for other parameters of the targets, thus indicating similar dose homogeneity and conformity for the two approaches. The mean DVH curves comparison for every target between MPs and APs of the three anatomical sites are provided in Additional file Fig. 3, Additional file Fig. 4, and Additional file Fig. 5.

Table 2
Comparison of dosimetric parameters between automated and manual plans for the targets of three anatomical sites.

Site	Item	Parameter	AP (M ± SD)	MP (M ± SD)	P
NPC	PGTV + nd	$D_{2\%}$ (Gy)	62.62 ± 0.53	63.43 ± 0.99	0.01
		$D_{98\%}$ (Gy)	60.04 ± 0.56	59.71 ± 1.28	0.19
		HI	0.043 ± 0.013	0.062 ± 0.026	< 0.01
		CI	0.763 ± 0.059	0.747 ± 0.083	0.73
	PTV1	$D_{2\%}$ (Gy)	62.43 ± 0.57	63.10 ± 0.92	0.01
		$D_{98\%}$ (Gy)	55.98 ± 1.14	55.39 ± 1.41	0.01
		HI	0.115 ± 0.023	0.138 ± 0.031	< 0.01
	PTV2	$D_{2\%}$ (Gy)	60.45 ± 2.95	60.64 ± 3.34	0.44
		$D_{98\%}$ (Gy)	50.14 ± 1.38	49.71 ± 1.39	0.02
		HI	0.204 ± 0.067	0.217 ± 0.076	0.08
ESCA	PTV	$D_{2\%}$ (Gy)	53.79 ± 0.46	53.77 ± 0.69	0.92
		$D_{98\%}$ (Gy)	49.21 ± 0.47	49.27 ± 1.13	0.19
		HI	0.088 ± 0.016	0.086 ± 0.033	0.76
		CI	0.817 ± 0.031	0.828 ± 0.038	0.16
RECA	PTV	$D_{2\%}$ (Gy)	52.49 ± 0.49	52.74 ± 0.52	0.06
		$D_{98\%}$ (Gy)	49.88 ± 0.14	49.79 ± 0.19	0.08
		HI	0.054 ± 0.009	0.061 ± 0.011	0.03
		CI	0.878 ± 0.031	0.903 ± 0.024	0.05

OARs Sparing

Table 3 reports the dose metrics for the OARs sparing of three anatomical sites. For NPC case, the max dose received by both lens, eyes and optic nerves in the APs is obviously lower than those in the MPs ($P < 0.01$), and the max dose was decreased by 16.8% (0.97 Gy), 15.7% (0.95 Gy), 28.6% (5.73 Gy), 30.7% (5.93 Gy), 19.2% (6.76 Gy) and 18.9% (6.93 Gy), respectively. The integral dose delivered to non-tumor tissues was significantly lower for APs than for the MPs, with a reduction of 2.7% ($p < 0.01$). No significant differences were found for the max dose of brain stem, spinal cord, chiasma and the mean dose, V30 of both parotids. For ESCA case, no significant differences were found for the V5 of both lungs and max dose of spinal cord. The V20, mean dose of both lungs and V30, V40, mean dose of heart in the

APs is lower than those in the MPs. For left and right lungs, the APs reduced the dose by 1.1% and 1.3% in V20, 3.5% (0.37 Gy) and 3.9% (0.38 Gy) in mean dose ($P < 0.05$). As for heart, APs yielded V30, V40 and mean dose lower by 5.1%, 3.0% and 8.7% (1.41 Gy) ($P < 0.05$), respectively. The integral dose was found lower with the APs, with a reduction of 2.7% with respect to MPs ($P < 0.05$). For RECA case, there was no significant difference in bladder sparing and integral dose between two approaches. The V30, V50 and mean dose of bowel in APs were decreased by 4.7%, 1.9% and 6.4% (1.27 Gy), respectively, and all the difference was statistically significant ($P < 0.05$). For the left and right femoral heads, the V30 were significantly lower in AP plan, with the reductions of 4.6% and 3.5% ($P < 0.05$), and the mean dose was decreased by 9.3% (1.6 Gy, $P < 0.05$) and 7.0% (1.2 Gy, $P > 0.05$), respectively. In addition to the parameters listed in Table 3, the more detailed DVH curves comparison for erery OAR is shown in Additional file file. Figure 2 shows the AP and MP plan isodose distributions for three representative patients with NPC, ESCA and RECA respectively. Figure 3 shows the box-plots of relative percentage differences in dose metric parameters for the main OARs between APs and MPs.

Table 3
Comparison of dosimetric parameters between automated and manual plans for the OARs of three anatomical sites.

Site	Item	Parameter	AP (M ± SD)	MP (M ± SD)	P
NPC	Brain stem	D_{max} (Gy)	44.82 ± 5.53	46.46 ± 4.00	0.14
	Spinal cord	D_{max} (Gy)	35.27 ± 3.95	36.21 ± 3.25	0.26
	Lens-L	D_{max} (Gy)	4.81 ± 1.77	5.78 ± 1.24	< 0.01
	Lens-R	D_{max} (Gy)	5.10 ± 1.89	6.05 ± 1.11	< 0.01
	Optic nerve-L	D_{max} (Gy)	28.48 ± 18.35	35.24 ± 15.18	< 0.01
	Optic nerve-R	D_{max} (Gy)	29.79 ± 17.23	36.72 ± 14.41	< 0.01
	Chiasma	D_{max} (Gy)	35.59 ± 16.86	40.10 ± 13.43	0.06
	Eye-L	D_{max} (Gy)	14.32 ± 6.48	20.05 ± 4.71	< 0.01
	Eye-R	D_{max} (Gy)	13.37 ± 5.70	19.30 ± 4.13	< 0.01
	Parotid-L	V30 (%)	42.64 ± 5.13	43.10 ± 5.37	0.73
		D_{mean} (Gy)	30.23 ± 2.42	30.27 ± 3.09	0.85
	Parotid-R	V30 (%)	43.47 ± 4.41	44.43 ± 3.27	0.41
		D_{mean} (Gy)	30.41 ± 2.68	30.73 ± 1.89	0.68
	ID	$Gy*cc*10^5$	1.42 ± 0.31	1.46 ± 0.27	0.03
ESCA	Lung-L	V5 (%)	49.69 ± 10.21	48.42 ± 6.91	0.24
		V20 (%)	18.77 ± 4.82	19.87 ± 5.36	0.03
		D_{mean} (Gy)	10.31 ± 2.36	10.68 ± 2.14	0.01
	Lung-R	V5 (%)	46.62 ± 8.46	46.65 ± 7.64	0.97
		V20 (%)	15.18 ± 5.72	16.44 ± 5.87	0.02
		D_{mean} (Gy)	9.45 ± 2.18	9.83 ± 2.30	< 0.01
	Heart	V30 (%)	15.93 ± 11.18	21.03 ± 13.94	< 0.01
		V40 (%)	8.21 ± 6.75	11.17 ± 8.60	< 0.01
		D_{mean} (Gy)	14.73 ± 7.60	16.14 ± 7.93	< 0.01
	Spinal cord	D_{max} (Gy)	36.15 ± 6.46	35.39 ± 8.15	0.32

Site	Item	Parameter	AP (M ± SD)	MP (M ± SD)	P
	ID	$Gy*cc*10^5$	1.47 ± 0.41	1.51 ± 0.42	< 0.01
RECA	Bladder	V20 (%)	93.8 ± 12.11	95.7 ± 8.9	0.62
		V50 (%)	30.6 ± 13.0	31.1 ± 13.2	0.73
		D_{mean} (Gy)	41.39 ± 5.9	41.13 ± 4.50	0.84
	Bowel	V30 (%)	25.71 ± 10.41	30.42 ± 11.26	< 0.01
		V50 (%)	9.74 ± 6.65	11.67 ± 7.60	< 0.01
		D_{mean} (Gy)	18.45 ± 5.23	19.72 ± 5.60	0.01
	Femoral Head-L	V30 (%)	12.24 ± 4.61	16.85 ± 8.65	0.01
		D_{mean} (Gy)	15.55 ± 2.61	17.15 ± 3.71	0.03
	Femoral Head-R	V30 (%)	12.74 ± 6.00	16.23 ± 8.26	< 0.01
		D_{mean} (Gy)	15.99 ± 2.95	17.17 ± 3.64	0.08
	ID	$Gy*cc*10^5$	2.21 ± 0.39	2.27 ± 0.41	0.07

Planning Efficiency and Dosimetric Verification

Table 4 reports a summary of the average MUs number, the total planning time, the beam-on time, and the results for dose delivery verification. For NPC and RECA cases, there were no significant differences in MUs and beam-on time between the APs and MPs. despite the MUs of APs is slightly increased by 3.6% (33 MUs) and 12.6% (59 MUs) than those of MPs, the beam-on time for the AP and MPs is similar for the two anatomical sites. While in the ESCA case, the MUs and beam-on time of APs is significantly lower than those of MPs.

Table 4
Summary of planning efficiency and treatment delivery metrics of automated and manual plans for the three anatomical sites.

Site	Parameter	AP (M ± SD)	MP (M ± SD)	P
NPC	MUs	670 ± 79	647 ± 121	0.51
	Beam-on time (s)	147 ± 34	143 ± 39	0.72
	Planning time (min)	40.3 ± 4.5	71.6 ± 15.8	< 0.01
	γ pass-rate (%)	97.5 ± 0.7	97.8 ± 0.7	0.11
ESCA	MU	467 ± 86	564 ± 106	< 0.01
	Beam-on time (s)	203 ± 24	215 ± 25	0.02
	Planning time (min)	10.8 ± 1.7	21.4 ± 4.2	< 0.01
	γ pass-rate (%)	98.0 ± 1.1	98.3 ± 0.9	0.5
RECA	MU	529 ± 154	470 ± 167	0.08
	Beam-on time (s)	127 ± 11	127 ± 12	0.85
	Planning time (min)	23.9 ± 1.9	53.2 ± 5.4	< 0.01
	γ pass-rate (%)	98.2 ± 0.9	98.1 ± 1.0	0.88

The planning time of the three anatomical sites was found to decrease dramatically in the transition from manual to automated planning. Compare with MP plans, AP plans for NPC, ESCA and RECA reduced the planning time by 43.7% (31.3 min), 49.5% (10.6 min), and 55.1% (29.3 min), respectively.

In order to assess the treatment accuracy, pre-treatment dosimetric verification was performed for all plans using the ArcCHECK phantom. With criteria equal to 3%-2 mm for gamma index, the plan passing rates were greater than 95% for all anatomical sites and techniques. Significant differences of the verification results between APs and MPs for all anatomical sites were not found.

Discussion

Manual planning is a time-consuming procedure, especially in busy clinical work, it is a great challenge to the planner. A clinically acceptable treatment plan requires experienced planner to manage a series of competing parameters on a patient basis, such as beam angle configuration, planning objectives. In order to improve the efficiency and quality of the treatment plans and provide better medical care for patients, a novel automated planning approach, Ruiplan, was developed in this study. Considering the complicated clinical application scenarios, this approach was designed feasible for multi-treatment techniques and multi-anatomical sites cancer treatment planning, it combines both benefits of atlas-based and template-based automated planning algorithm, with the functionalities of dose prediction, beam angle optimization, auxiliary structures automatic generation and objectives adaptively adjustment.

To demonstrate the clinical performance of the Ruiplan, comparative planning work was performed to compare the dose metric results of targets and OARs sparing for 60 randomly selected patients (NPC: 20, ESCA:20 and RECA:20). In the three anatomical sites, treatments involved large concave-shaped targets, multiple dose prescriptions, complicated target-OAR relationships, different treatment techniques, and therefore presented the most complex and challenging problems for plan optimization. Results of our work showed that the APs maintained similar or superior plan quality to the MPs. As shown the dosimetric parameters in Table 2 and boxplot of dosimetric difference in Fig. 3, the APs significantly improve dose homogeneity in the NPC and RECA cases, similar dose conformity in all anatomical sites. In terms of OARs sparing, the use of Ruiplan translated in a significant improvement in most of OARs sparing compared to the MPs in all anatomical sites. As shown in Table 3, the max dose of the lens, eyes and optic nerves in NPC case site, the V20 and mean dose of lungs, the V30, V40 and mean dose of heart in ESCA case, theV30, V50 and mean dose of bowel and the V30 of femoral heads in CRCA case were significantly decreased on average with APs compared to MPs. Moreover, the integral doses delivered to non-tumor tissues in three anatomical sites cancer were lower in APs, which means a lower risk of secondary malignancies [32]. From this point of view, the developed Ruiplan is robust under different anatomical sites, treatment techniques and prescription doses presented in this study.

Regarding planning and treatment efficiency, the APs resulted in 3.6% and 12.6% increase of MUs for the NPC and RECA cases with VMAT treatment technique, a higher MUs refers to an increase of plan complexity, this finding is in agreement with previous studies [11, 33, 34]. The increased plan complexity may lead to challenges in radiation delivery [35]. For the sake of determining the trade-off between plan complexity and dose delivery accuracy, pre-treatment dosimetric verification were performed for all the generated plans, no significant difference was observed between APs and MPs for the NPC and RECA cases in the dose verification. Moreover, the increase of MUs did not translate to a longer delivery time, which is reasonable because of in the VMAT delivery mode, Raystation tend to maintain the gantry rotation at a fixed speed and adjust the dose rate of each control point to modulate the dose distribution. Unlike the MUs increase in the APs of NPC and RECA cases, in the ESCA case, the APs use about 17.2% less MUs to achieve similar PTV coverage and superior OARs sparing comparing with the MPs. We believe that this phenomenon could probably to attributed to the adoption of BAO, which is capbale of finding an optimal beam angle configuration for the IMRT APs, similar results were also reported by Lin et al. [20]. A less MUs of IMRT plans resulted in a shorter delivery time which means a higher treatment efficiency, because in Raystation a static dose rate was used in IMRT delivery mode.

Many previous studies have shown that high efficiency is a significant feature of automated planning [13, 20, 23, 33], and this is also consistent with our work. As shown in Table 4, the average planning time needed for generating the AP plans was reduced by at least by 43% compared with manual work. The observed advantage of the automated planning implies that when applying a more complicated plan design, Ruiplan may not only save a great deal of time for planner, but also find acceptable or even better solutions for a standardized and optimized treatment plan than a planner could within a limited time. Every month, more than one hundred treatment plans mentioned in this work are planned in Henan Cancer Hospital, and this would be a daunting task if planned manually. Owing to the Ruiplan, dozens of

working hours will be saved per month. With the demonstrated efficiency increase, the medical physicists and dosimetrists would become capable of devoting a larger portion of time on other areas requiring innovation and creativity, such as individualized care, artificial intelligence (AI) based studies, and other activities which were not possible with conventional clinical practices [33]. Another potential advantage of automated planning is the absence of inter- and intra-planner variations, because even for the most experienced planner, time pressure to deliver a clinically applicable plan may result in treatment plans of inferior quality than desired. Furthermore, after automatic optimization, the APs can be further optimized if there are special clinical requirements.

To summarize, superiorities of the Ruiplan demonstrated in this study include the following. First, multi-treatment techniques and multi-anatomical sites were supported. Second, similar or superior plan quality compared to the MPs. Third, significant higher efficiency than manul planning.

There are several limitations in this study. First, the dose predict model used in this work was based on a multiple linear regression method, the prediction results of this model may not be as accurate as those of models based on AI methods. Second, no collimator angle optimization algorithms were used in this study. Further studies in the future are therefore needed to focus on more accurate dose prediction and collimator angle optimization, with an objective to improve the clinical performance of our automated planning approach.

Conclusion

A novel automated planning approach, Ruiplan, was developed in this work. This approach combines both benefits of atlas-based and template-based automated planning algorithm with its capability for multi-treatment techniques and multi-anatomical cancer radiotherapy. The APs generated by using Ruiplan were clinically acceptable treatment plans and comparable to the MPs manually generated by experienced physicist. This highlights potential of the Ruiplan for enhancing the efficiency of treatment planning process and the plan quality for radiotherapy, enabling hospital to allocate time, manpower and other resources in a more effective and efficient manner.

Abbreviations

IMRT: Intensity-modulated radiation therapy; VMAT: Volumetric-modulated arc therapy; SBRT: Stereotactic body radiation therapy; SRS: Stereotactic radiosurgery; BAO: Beam angle optimization; OAR: Organ at risk; DVH: Dose volume histogram; TPS: Treatment planning system; NPC: Nasopharyngeal carcinoma; ESCA: Esophageal carcinoma; RECA: Rectal cancer; AP: automated plan; MP: manual plan;CI: Conformity index; HI: Homogeneity index; MU: Monitor unit; AJCC: American Joint Committee on Cancer; DMPO: Direct machine parameter optimization;ID: Integral dose; AI: Artificial intelligence.

Declarations

Acknowledgments

Not applicable.

Availability of data and materials

The Ruiplan code during the current study are available from ZY Lou (louslove@163.com) to any reader directly on reasonable request.

Authors' contributions

ZYL and LLT designed the automated planning algorithm. RHM, DJL and BLcollected the data, performed the statistical analysis. ZYL and BL wrote the manuscript. HCL and HG revised and approved the final manuscript. All authors read and approved the final manuscript.

Ethics approval and consent to participate

The study was approved by the Institutional Review Board of the affiliated cancer hospital of Zhengzhou University.

Consent for publication

Not applicable.

Competing interests

The authors declare that they have no competing interests.

Funding

This work was supported in part by the National Natural Science Foundation of China (No. 81773230) and the Joint Construction Project of Henan Medical Science and Technology Research Program in 2019 (LHGJ20190661).

References

1. Bohsung J, Gillis S, Arrans R, Bakai A, De Wagter C, Knoos T, et al. IMRT treatment planning:- a comparative inter-system and inter-centre planning exercise of the ESTRO QUASIMODO group. Radiother Oncol. 2005;76:354-61.
2. Hussein M, Heijmen BJM, Verellen D, Nisbet A. Automation in intensity modulated radiotherapy treatment planning-a review of recent innovations. Br J Radiol. 2018;91:20180270.
3. Powis R, Bird A, Brennan M, Hinks S, Newman H, Reed K, et al. Clinical implementation of a knowledge based planning tool for prostate VMAT. Radiat Oncol. 2017;12:81.

4. Fan J, Wang J, Chen Z, Hu C, Zhang Z, Hu W. Automatic treatment planning based on three-dimensional dose distribution predicted from deep learning technique. Med Phys. 2019;46:370-81.
5. Peng J, Chen Y, Zhao J, Wang J, Xia X, Cai B, et al. An atlas-guided automatic planning approach for rectal cancer intensity-modulated radiotherapy. Phys Med Biol. 2021;66.
6. Fogliata A, Reggiori G, Stravato A, Lobefalo F, Franzese C, Franceschini D, et al. RapidPlan head and neck model: the objectives and possible clinical benefit. Radiat Oncol. 2017;12:73.
7. Chatterjee A, Serban M, Abdulkarim B, Panet-Raymond V, Souhami L, Shenouda G, et al. Performance of Knowledge-Based Radiation Therapy Planning for the Glioblastoma Disease Site. Int J Radiat Oncol Biol Phys. 2017;99:1021-28.
8. Hussein M, South CP, Barry MA, Adams EJ, Jordan TJ, Stewart AJ, et al. Clinical validation and benchmarking of knowledge-based IMRT and VMAT treatment planning in pelvic anatomy. Radiother Oncol. 2016;120:473-79.
9. Hof SV, Delaney AR, Tekatli H, Twisk J, Slotman BJ, Senan S, et al. Knowledge-Based Planning for Identifying High-Risk Stereotactic Ablative Radiation Therapy Treatment Plans for Lung Tumors Larger Than 5 cm. Int J Radiat Oncol Biol Phys. 2019;103:259-67.
10. Wu H, Jiang F, Yue H, Zhang H, Wang K, Zhang Y. Applying a RapidPlan model trained on a technique and orientation to another: a feasibility and dosimetric evaluation. Radiat Oncol. 2016;11:108.
11. Cilla S, Ianiro A, Romano C, Deodato F, Macchia G, Buwenge M, et al. Template-based automation of treatment planning in advanced radiotherapy: a comprehensive dosimetric and clinical evaluation. Sci Rep. 2020;10:423.
12. Ge Y, Wu QJ. Knowledge-based planning for intensity-modulated radiation therapy: A review of data-driven approaches. Med Phys. 2019;46:2760-75.
13. Sheng Y, Li T, Yoo S, Yin FF, Blitzblau R, Horton JK, et al. Automatic Planning of Whole Breast Radiation Therapy Using Machine Learning Models. Front Oncol. 2019;9:750.
14. Castriconi R, Esposito PG, Tudda A, Mangili P, Broggi S, Fodor A, et al. Replacing Manual Planning of Whole Breast Irradiation With Knowledge-Based Automatic Optimization by Virtual Tangential-Fields Arc Therapy. Front Oncol. 2021;11:712423.
15. Voet PW, Breedveld S, Dirkx ML, Levendag PC, Heijmen BJ. Integrated multicriterial optimization of beam angles and intensity profiles for coplanar and noncoplanar head and neck IMRT and implications for VMAT. Med Phys. 2012;39:4858-65.
16. Xia P, Murray E. 3D treatment planning system-Pinnacle system. Med Dosim. 2018;43:118-28.
17. Zarepisheh M, Hong L, Zhou Y, Oh JH, Mechalakos JG, Hunt MA, et al. Automated intensity modulated treatment planning: The expedited constrained hierarchical optimization (ECHO) system. Med Phys. 2019;46:2944-54.
18. Xhaferllari I, Wong E, Bzdusek K, Lock M, Chen J. Automated IMRT planning with regional optimization using planning scripts. J Appl Clin Med Phys. 2013;14:4052.

19. Hernandez Morales D, Shan J, Liu W, Augustine KE, Bues M, Davis MJ, et al. Automation of routine elements for spot-scanning proton patient-specific quality assurance. Med Phys. 2019;46:5-14.
20. Lin TC, Lin CY, Li KC, Ji JH, Liang JA, Shiau AC, et al. Automated Hypofractionated IMRT treatment planning for early-stage breast Cancer. Radiat Oncol. 2020;15:67.
21. Zhang X, Li X, Quan EM, Pan X, Li Y. A methodology for automatic intensity-modulated radiation treatment planning for lung cancer. Phys Med Biol. 2011;56:3873-93.
22. Ayala R, Ruiz G, Valdivielso T. Automatizing a nonscripting TPS for optimizing clinical workflow and reoptimizing IMRT/VMAT plans. Med Dosim. 2019;44:409-14.
23. Yang Y, Shao K, Zhang J, Chen M, Chen Y, Shan G. Automatic Planning for Nasopharyngeal Carcinoma Based on Progressive Optimization in RayStation Treatment Planning System. Technol Cancer Res Treat. 2020;19:1533033820915710.
24. Han EY, Kim GY, Rebueno N, Yeboa DN, Briere TM. End-to-end testing of automatic plan optimization using RayStation scripting for hypofractionated multimetastatic brain stereotactic radiosurgery. Med Dosim. 2019;44:e44-e50.
25. Okada H, Ito M, Minami Y, Nakamura K, Asai A, Adachi S, et al. Automatic one-click planning for hippocampal-avoidance whole-brain irradiation in RayStation. Med Dosim. 2021.
26. Mayo CS, Moran JM, Bosch W, Xiao Y, McNutt T, Popple R, et al. American Association of Physicists in Medicine Task Group 263: Standardizing Nomenclatures in Radiation Oncology. Int J Radiat Oncol Biol Phys. 2018;100:1057-66.
27. Pang H, Sun X, Yang B, Wu J. Predicting the dose absorbed by organs at risk during intensity modulated radiation therapy for nasopharyngeal carcinoma. Br J Radiol. 2018;91:20170289.
28. Kataria T, Sharma K, Subramani V, Karrthick KP, Bisht SS. Homogeneity Index: An objective tool for assessment of conformal radiation treatments. J Med Phys. 2012;37:207-13.
29. Feuvret L, Noel G, Mazeron JJ, Bey P. Conformity index: a review. Int J Radiat Oncol Biol Phys. 2006;64:333-42.
30. Li G, Zhang Y, Jiang X, Bai S, Peng G, Wu K, et al. Evaluation of the ArcCHECK QA system for IMRT and VMAT verification. Phys Med. 2013;29:295-303.
31. Miften M, Olch A, Mihailidis D, Moran J, Pawlicki T, Molineu A, et al. Tolerance limits and methodologies for IMRT measurement-based verification QA: Recommendations of AAPM Task Group No. 218. Med Phys. 2018;45:e53-e83.
32. Newhauser WD, Berrington de Gonzalez A, Schulte R, Lee C. A Review of Radiotherapy-Induced Late Effects Research after Advanced Technology Treatments. Front Oncol. 2016;6:13.
33. Cilla S, Romano C, Morabito VE, Macchia G, Buwenge M, Dinapoli N, et al. Personalized Treatment Planning Automation in Prostate Cancer Radiation Oncology: A Comprehensive Dosimetric Study. Front Oncol. 2021;11:636529.
34. Buschmann M, Sharfo AWM, Penninkhof J, Seppenwoolde Y, Goldner G, Georg D, et al. Automated volumetric modulated arc therapy planning for whole pelvic prostate radiotherapy. Strahlenther

Onkol. 2018;194:333-42.

35. Wall PDH, Fontenot JD. Evaluation of complexity and deliverability of prostate cancer treatment plans designed with a knowledge-based VMAT planning technique. J Appl Clin Med Phys. 2020;21:69-77.

Figures

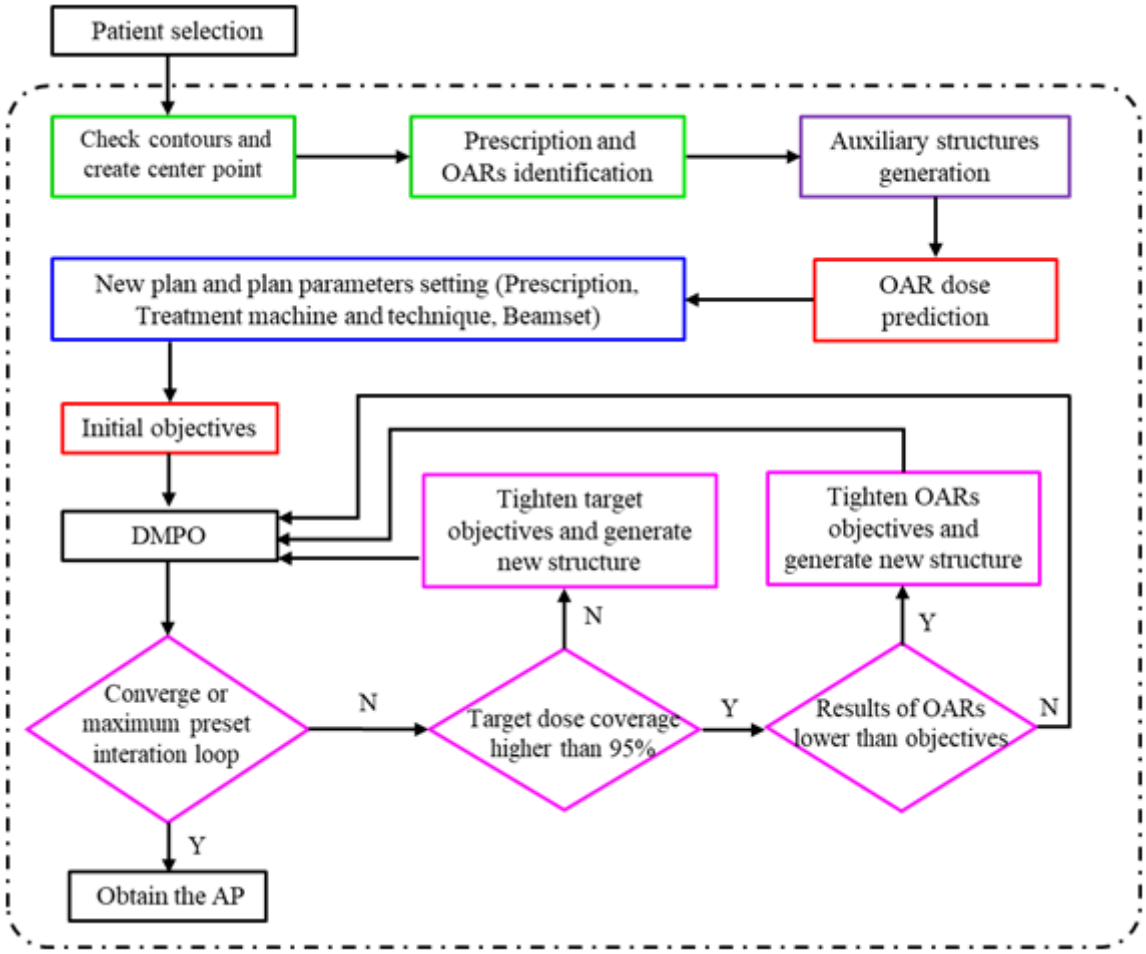

Figure 1

The workflow of Ruiplan.Green part indicates the prescription and OAR identification module, purple part indicates the auxiliary structure generate module, red part indicates thedose prediction and objectives setting module, blue part indicates the beam configuration module, pink part indicates the plan fine tuning module.

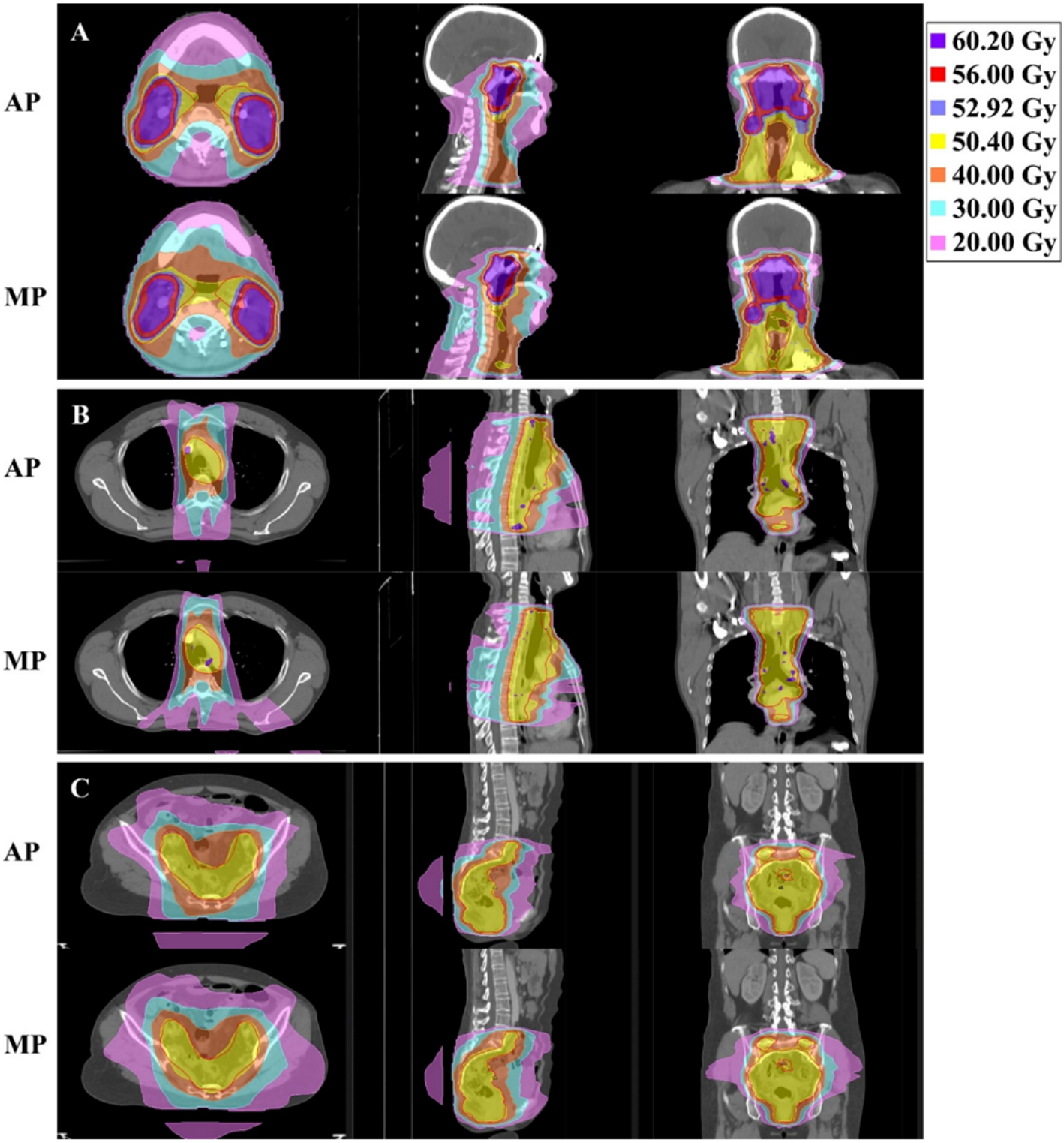

Figure 2

Dose distributions in three representative patients for automated plan (AP) and manual plan (MP).Row (A)for NPC patient, row (B) for ESCA patient androw (C) for RECA patient.

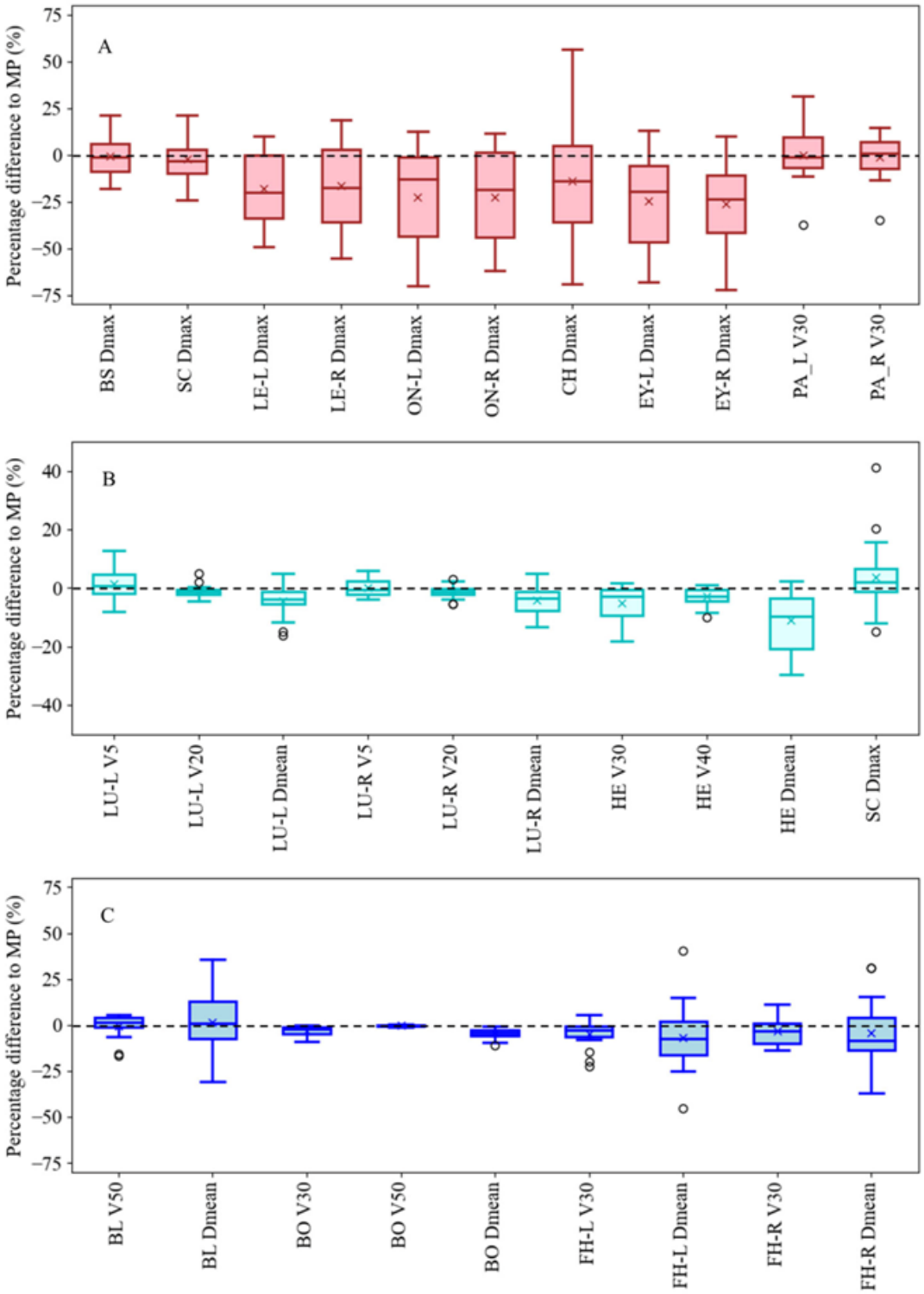

Figure 3

Boxplots of differences of the main dosimetric of automated plans compared to manual plans. Negative difference indicates better OARsparing for automated plans. Row (A) for NPC patients, row (B) for ESCA patients and row (C) for RECA patients. the edges of the box are the 25th and 75th percentiles, the crosses represent the mean values,black circles represent the extreme values. Abbreviations: BS, brain

stem; SC, spinal cord; LE, lens; ON, optic nerve; CH, chiasma; EY, eye; PA, parotid; LU, lung; HE, heart; BL, bladder; BO, bowel; FH, femoral head.

Supplementary Files

This is a list of supplementary files associated with this preprint. Click to download.

- Additionalfile.docx